Unbinding–Binding Transition Induced by Molecular Snaps in Model Membranes

N. Taulier,* C. Nicot,* M. Waks,* R. S. Hodges,† R. Ober,‡ and W. Urbach§

*Laboratoire d'Imagerie Paramétrique, UMR 7623 CNRS, Université Pierre et Marie Curie, 15 rue de l'Ecole de Médecine, 75270 Paris cédex 06, France, †University of Alberta, Department of Biochemistry, 321A Medical Sciences Building, Edmonton, Alberta T6G 2H7, Canada, ‡Laboratoire de la Matière Condensée, URA 792 CNRS, Collège de France, 10 Place Marcelin Berthelot, 75005 Paris, France, and §Laboratoire de Physique Statistique, UMR 8550 CNRS, Ecole Normale Supérieure, 24 rue Lhomond, 75231 Paris cédex 05, France

ABSTRACT We have used a lamellar phase made of a nonionic surfactant, dodecane and water, as a model membrane to investigate its interactions with macromolecular inclusions bringing together two membranes, i.e., acting as macromolecular snaps. In systems devoid of inclusions, the interlamellar distance depends on the total volume fraction of membranes Φ. We show that, in presence of a transmembrane protein, or of several *de novo* designed peptides of different length and composition, the lamellar phase undergoes a binding transition. Under such conditions, the interlamellar distance is no longer proportional to Φ^{-1}, but rather to the surface concentration of snaps within the membrane. It also appears that, in the presence of the hydrophobic segment of peptide snaps, the length of the inclusions must be at least equal to the hydrophobic length of the membrane to be active. Experimental results have been precisely fitted to a model of thermally stabilized membranes, decorated with snaps. However, in the presence of inclusions, the parameter describing the interactions between membranes, has to take into account the length of the inclusion to preserve good predictive capabilities.

INTRODUCTION

A lamellar phase L_α is a stack of membranes made of amphiphilic molecules separated by a solvent. The interactions of dilute lamellar phases with macromolecules have been documented in the last few years. These macromolecules can be located in different loci of a membrane whether confined within bilayers or adsorbed on their surface, they can modify significantly inter- or intramembrane interactions. Such interactions have been discussed theoretically (Daoud and de Gennes, 1977; Brooks and Cates, 1993) and confirmed experimentally (Bouglet and Ligoure, 1999). However, most of these models have been applied to polymers displaying a Gaussian-like structure in bulk.

In the present work, we have been interested in more organized inclusions and their interactions with lamellar phases. Indeed, peptides and proteins have known sequences, they display a well-defined periodic structure such as α-helices, and they are monodisperse. Furthermore, they constitute a biologically relevant experimental material. A number of theoretical papers have attempted to describe the behavior of such inclusions, in particular, the intricate interactions of proteins and lipids in membranes or in complex fluids, considered as membrane-mimetic systems (reviewed by Abney and Owicki, 1985; Marcelja, 1999). In the literature, the size of the inclusions is, in general, of the same order of magnitude as the bilayer itself. We have investigated a different experimental situation, where the size of the inserted protein is larger than that of the studied bilayer. Although specific interrelations between the intramembrane domains of proteins and peptides with the surrounding lipids have been extensively documented, the details of peptide chain interaction with the bilayer require additional insights. They are crucial for the understanding of the membrane architecture and for the stability of the active conformation of membrane proteins that control a wide array of vital functions.

Less studied nonionic surfactant systems constitute appropriate, although simplified, models of biological significance, by avoiding long-range electrostatic interactions occurring with ionic surfactants, often responsible of protein destabilization (Honig and Nicholls, 1995). Moreover polyethylene glycol alkyl ether ternary systems offer a rich phase behavior, where the lamellar phases are dominated by Helfrich repulsion forces. In the present work, we have selected ternary systems that display L_α phases in a temperature range, compatible with stable native protein conformation (Merdas et al., 1996, 1998). As shown in Fig. 1, the lamellar phase is composed of a water layer interposed between two surfactant monolayers (reverse membrane), separated by the swelling oil. Under well-defined conditions, we have observed the spontaneous insertion of hydrophobic peptides, leading to a two-phase transition: an upper oil phase and an inclusion-containing L_α phase. These inclusions can act as molecular snaps (Fig. 1) that bring together two surfactant monolayers, inducing a corresponding decrease of the Bragg distance. By doing so, one could say that such inclusions create a normal water-swollen membrane.

To shed light on the snap insertion mechanism, we have systematically investigated a series of synthetic membrane-

Received for publication 23 June 1999 and in final form 16 November 1999.

Address reprint requests to Wladimir Urbach, Laboratoire de Physique Statistique, UMR 8550 CNRS, Ecole Normale Supérieure, 24 rue Lhomond, 75231 Paris cédex 05, France. Tel.: 33-144-3234-19; Fax: 33-144-3234-33; Email: urbach@physique.ens.fr.

0006-3495/00/02/857/09 $2.00

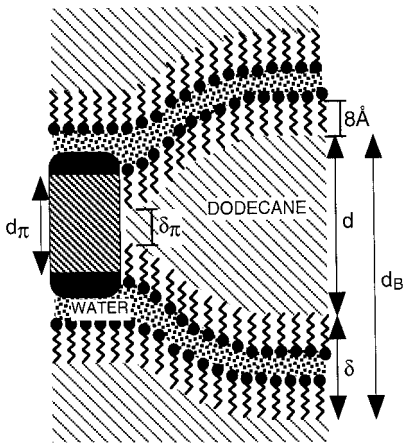

FIGURE 1 Diagram of a molecular snap embedded in a reverse lamellar phase. The hydrophobic length of the snap is d_π and the length of its hydrophobic part in contact with oil is δ_π. The periodicity d_B of the lamellar phase is the sum of the mean distance between membranes, d, and the bilayer thickness δ.

interacting, hydrophobic peptides of variable length and various composition. We have compared the results that those obtained with a transmembrane protein, previously studied by us (Nicot et al., 1996): the Folch-Pi myelin proteolipid, involved in demyelinating diseases (Greer et al., 1996). By the interplay between the hydrophobic nature of peptide sequences and their length, it is possible to identify and to optimize the threshold conditions for bilayer crossing and snap-like effect.

We have used the Helfrich approach to characterize the various physical parameters of the lamellar phase without inclusion (unbound state) and to analyze our data. Their comparison with those obtained in presence of inclusions (bound state) has allowed us to provide a theoretical explanation of the observed mechanism in possible relation with similar biological processes.

MATERIALS AND METHODS

Chemicals and ternary system

Tetraethylene glycol monododecyl ether (NIKKOL BL-4SY), denoted $C_{12}E_4$, was obtained from Nikko Chemicals Co. Ltd. (Tokyo, Japan). Tetraethylene glycol monodecyl ether, denoted $C_{10}E_4$, was from Sigma (St. Louis, MO, USA). Anhydrous dodecane was purchased from Aldrich Chemical Co. (Milwaukee, WI, USA) and isooctane Pro analysi grade, from Merck (Darmstadt, Germany). Water was of MILLIQ type (Millipore S.A., Molsheim, France).

The $C_{12}E_4$–water–dodecane system displays at low water content, a wide and stable L_α reverse phase, at room temperature (Kunieda et al., 1991; Merdas et al., 1996). The reverse lamellar phase (Fig. 1) has been investigated at two different values of water thickness, defined as water-to-surfactant volume ratios $w = 0.58$ and 0.98, and at various membrane volume fraction Φ. In contrast, the $C_{10}E_4$–dodecane–water system displays a very narrow lamellar phase. The smallest possible Φ was found to be $\Phi = 0.29$ with $w = 0.45$.

Molecular inclusions

Myelin proteolipid

The proteolipid was purified from bovine brain as described elsewhere (Vacher et al., 1989). In the present work, a slight modification was carried out as follows: after the first isooctane precipitation, the proteolipid, spun at 1000 rpm, was suspended in an excess of hexane large enough to remove the remaining traces of isooctane. It was spun at 3500 rpm at 4°C for 10 min and dissolved in a mixture of chloroform-methanol 2/1 (volume/volume). We have shown previously (Vacher et al., 1989) that, under the above experimental conditions, about 10 lipid molecules remain tightly bound to one protein molecule. Furthermore, thiol groups are preserved, as well as thioester linkages between thiol groups and six covalently bound fatty acid molecules, found crucial for preservation of the native conformation. In addition to the presence of fatty acids, the amino acid composition makes this protein one of the most hydrophobic found in the literature (Weimbs and Stoffel, 1992). Its four transmembrane α-helices are composed of 27–29 amino acids and correspond to an average length of 42 Å per hydrophobic helix.

Synthetic Peptides

We have investigated the behavior of a series of hydrophobic peptides of various length of known α-helical structure (Davis et al., 1983; Liu and Deber, 1997). Two of them were made less hydrophobic by the introduction of alanine residues into their sequence. The peptides Lys-Lys-$(Ala)_3$-Leu-$(Ala)_4$-Leu-$(Ala)_2$-Trp-$(Ala)_2$-Leu-$(Ala)_3$-$(Lys)_4$-Amide, denoted (Ala-Leu 18), and Lys-Lys-Gly-$(Leu)_8$-Lys-Lys-Ala-Amide, denoted $(Leu)_8$, were obtained from Neosystems (Strasbourg, France). The peptides Ac-Lys-Lys-Gly-$(Ile\text{-}Ala)_4$-Lys-Lys-Ala-Amide denoted $(Ile\text{-}Ala)_4$, Ac-Lys-Lys-Gly-$(Leu)_{12}$-Lys-Lys-Ala-Amide denoted $(Leu)_{12}$, and Lys-Lys-Gly-$(Leu)_{16}$-Lys-Lys-Ala-Amide denoted $(Leu)_{16}$ were synthesized according to Sereda et al. (1993). By assuming that all the residues in an α-helical conformation have an amino acid residue translation of 1.5 Å per residue (Cantor and Schimmel, 1980), the length of the peptides is 27, 12, 12, 18, and 24 Å, respectively.

Sample preparation

The sample preparation is the same for the proteolipid and the various peptides. The macromolecule and the surfactant both in chloroform-methanol solution, are mixed in appropriate ratios, evaporated to dryness under a stream of nitrogen, and further dried under vacuum over phosphorous pentoxide for three hours. The solubilization of the macromolecule is carried out at 32°C, in $C_{12}E_4$ by adding a weighed amount of dodecane and water to the dessicated mixtures. Few minutes of sonication at that temperature are sufficient to obtain an isotropic, optically clear, reverse micellar solution, ready for a spectroscopic measurement of protein concentration. The transition to the lamellar phase is obtained by lowering the temperature under 29°C. After 7 days of equilibrium at 20–22°C, the volume of dodecane expelled from the L_α phase reaches its maximum, and a new lamellar phase is ready for measurements.

In the $C_{10}E_4$ ternary system, the myelin proteolipid can be solubilized in the reverse micellar phase above 34°C. However, after lowering the temperature, the phase diagram of the system becomes different from that of $C_{12}E_4$: a two-phase system is then observed between the micellar and lamellar phases (20–22°C), leading to the precipitation of the proteolipid. In contrast, under similar conditions, the hydrophobic peptides remain soluble.

Small angle x-ray Scattering

The L_α phase is transferred in Mark-Röhrchen capillaries of 1.5 mm diameter and sealed. The x-ray generator was a copper rotating anode

machine operating at 40 kV and 25 mA. The x-ray apparent source had dimensions 0.1 × 0.1 mm. A vertical mirror acts as a total reflector for the $\lambda_{K\alpha} = 1.54$ Å wavelength, eliminates shorter wavelengths of the beam, and directs the x-rays on the positive proportional counter. A nickel filter attenuates the K_β wavelength. The dimensions of the beam on the counter were 3 mm vertically and 0.3 mm horizontally. The counter had a window of 3 mm height, a 50 mm useful length and a 200 μm spatial resolution. The distance between the sample and the counter was 802 mm. The measurements were carried out at 20–22°C. Small angle x-ray scattering (SAXS) data were analyzed using the general equation for the scattered intensity derived by Nallet et al. (1993).

THEORETICAL BACKGROUND

SAXS

This type of experiments yields essential information concerning the structure and elastic constants of the studied phase. The repetition Bragg distance d_B in a lamellar phase is obtained from peak position q_0,

$$d_B = \frac{2\pi}{q_0}.$$

In the peak vicinity, the signal varies as $|q - q_0| = I^{1-\eta}$ where the Caillé (1972) exponent η is defined as

$$\eta = \frac{\pi k_B T}{2 d_B^2 \sqrt{K\bar{B}}}, \tag{1}$$

where $\bar{B}$ describes interlamellar interactions and K is related to κ, the bending constant of a single membrane, by the relation $K = \kappa/d_B$.

Both elastic parameters can be deduced by fitting the x-ray spectra (Roux and Safinya, 1988; Lei et al., 1995; Nallet et al., 1993). In this work, we have selected the approach of Nallet et al. (1993), which allows the calculation of η, d_B, and the thickness of the polar part of the membrane. We have added 16 Å to the polar part (water and headgroup) of the membrane, representing the length of two $C_{12}E_4$ surfactant tails (Klose et al., 1995) to obtain the total membrane thickness δ (Fig. 1). This approach leads to the δ_{RX} values in Tables 1 and 3.

Dilution law

For an undeformed flat membrane, its surface coincides with the x–y plane. Then a simple geometrical model shows that the variation of d_B with Φ the membrane volume fraction in the sample, is connected to δ by

$$d_B = \frac{\delta}{\Phi}.$$

For a flexible membrane, its true area S does not coincide with its projection on the x–y base, S_B. The dilution law must then be written as

$$d_B = \frac{\delta}{\Phi}\frac{S}{S_B}.$$

For a rigid membrane $S_B = S$ and for a flexible membrane (Helfrich, 1985),

$$\frac{S}{S_B} = 1 + \frac{k_B T}{2\pi\kappa}\ln\left(\frac{\xi_\parallel}{a}\right),$$

where a is the surfactant molecular dimension (Golubovic and Lubensky, 1989), and

$$\xi_\parallel = \sqrt{\frac{32}{3\pi}}\sqrt{\frac{\kappa}{k_B T}}(d_B - \delta)$$

is related to the largest wavelength of the fluctuating membrane. The dilution law becomes then (Roux et al., 1992)

$$d_B = \frac{\delta}{\Phi}(\alpha - \beta \ln \Phi), \tag{2}$$

where

$$\alpha = 1 + \frac{k_B T}{4\pi\kappa}\ln\left(\sqrt{\frac{32\kappa}{3\pi k_B T}}\frac{\delta}{a}\right)$$

and

$$\beta = \frac{k_B T}{4\pi\kappa}.$$

The fit of Eq. 2 allows the estimation of κ.

Binding transition in a lamellar phase including snaps

Lyotropic lamellar phases can be found in bound or unbound states (Leibler and Lipowsky, 1987; Sens et al., 1997). The transition between the two states can be driven, for instance, by van der Waals interactions. Below a critical value of these interactions, the lamellar phase is unbound and the intermembrane distance is fixed by the global concentration of membranes. If van der Waals interactions are above the critical value, a bound lamellar phase is observed, and the intermembrane spacing is fixed by the balance between the van der Waals interactions and the Helfrich repulsion between membranes. In the present work, we have observed a transition to the bound state induced by molecular snaps. When snaps are added to a lamellar oil-swollen phase, we observe that, after a lag period, an upper oil phase forms on the top of the snap-containing L_α phase.

In the following section, we describe the classic Helfrich theory, which we will further extend to take into account the presence of snaps in the membrane.

Periodicity of an unbound lamellar phase

We first consider a stack of membranes of zero thickness and of surface S, at a distance d from each other. In Monge's representation, the reference plane of a membrane is taken parallel to the plane xy. In the unbinding form (van der Waals interactions cannot overcome the repulsion), the thermal fluctuations around such plane are described by the displacement vector $u(\vec{r})$ along the z axis. Two characteristic lengths are associated with these fluctuations (Gompper and Schick, 1994):

- $\xi_\perp$ measures the mean fluctuation amplitude along the z axis. This parameter is equal to the mean amplitude of displacement $\xi_\perp = \sqrt{\langle u^2(\vec{r})\rangle}$.
- $\xi_\parallel$ is related to the largest wavelength of the fluctuating membrane.

The energy of this lamellar phase can be written

$$\mathrm{E} = \int\left[\frac{K}{2}\left(\frac{\partial^2 u(\vec{r})}{\partial x^2} + \frac{\partial^2 u(\vec{r})}{\partial y^2}\right)^2 + \frac{\bar{B}}{2}\left(\frac{\partial u(\vec{r})}{\partial z}\right)^2\right]\mathrm{d}^3\vec{r}. \quad (3)$$

A Fourier transform of the displacement,

$$u(\vec{r}) = \frac{1}{(2\pi)^3}\int u_\mathrm{q} e^{i\vec{q}\cdot\vec{r}}\mathrm{d}^3 q,$$

and the use of the equipartition theorem for each energy mode leads to the following expression of the mean quadratic value of u_q,

$$\langle |u_\mathrm{q}|^2\rangle = \frac{V}{(2\pi)^3 K}\frac{k_\mathrm{B}T}{q_\perp^4 + (1/\lambda^2)q_\parallel^2}, \quad (4)$$

where $\lambda = \sqrt{K/\bar{B}}$ is the smectic penetration length (de Gennes, 1974), and V is the volume of the lamellar phase.

The periodicity of the lamellar phase, characterized by the repetition distance, d, is reflected in the reciprocal space by a wave vector $q_\parallel$, which has the value of $q_0 = 2\pi/d$. Because $\mathrm{q}_\parallel = 0$ everywhere except for $q_\parallel = q_0$, the Parseval theorem gives after integration on $q_\parallel$:

$$\xi_\perp^2 = \int \langle u_\mathrm{q}^2\rangle\,\mathrm{d}\vec{q} = \frac{1}{2\pi\kappa}\int_{\pi/\sqrt{S}}^{\pi/a}\frac{k_\mathrm{B}T}{q_\perp^4 + \frac{1}{\lambda^2}\left(\frac{2\pi}{d}\right)^2}q_\perp\,\mathrm{d}q_\perp. \quad (5)$$

Integration of Eq. 5 leads to

$$\xi_\perp^2 = \frac{k_\mathrm{B}T}{4\pi^3\kappa}\frac{\pi}{2}\lambda d\left[\arctan\left(\left(\frac{1}{a}\right)^2\frac{\pi}{2}\lambda d\right) - \arctan\left(\frac{1}{S}\frac{\pi}{2}\lambda d\right)\right]. \quad (6)$$

A natural length $\xi_\parallel$ appears in the arctangent to obtain a dimensionless term. It differs from the value found by de Gennes (1974) by $\sqrt{\pi/2}$,

$$\xi_\parallel = \sqrt{\frac{\pi}{2}\lambda d}. \quad (7)$$

Taking into account (Helfrich and Servuss, 1984)

$$\xi_\perp \approx \frac{d}{\sqrt{6}}, \quad (8)$$

Eq. 6 becomes

$$d^2 = \frac{3k_\mathrm{B}T}{2\pi^3\kappa}\xi_\parallel^2\left[\arctan\left(\frac{\xi_\parallel^2}{a^2}\right) - \arctan\left(\frac{\xi_\parallel^2}{S}\right)\right]. \quad (9)$$

The terms between brackets take into account the contribution of surrounding membranes, and constitute a correction of the equation established by Nicot et al. (1996). If we consider a membrane of finite thickness δ and periodicity d_B, the distance between two neighboring membranes will be $d = d_\mathrm{B} - \delta$. Now, we will consider the presence of an inclusion.

Periodicity of a bound lamellar phase

For a low surface concentration of snaps, C, the average distance between two inclusions, ℓ, does not impose any cut-off on the fluctuating membrane wavelength. The expression of d (Eq. 9) remains valid, and it is expected that d and d_B also remain independent of C. In contrast, when C increases, then ℓ becomes the pertinent length as soon as it becomes smaller or equal to the largest wavelength of the fluctuating membrane. As a consequence, the presence of molecular snaps will prevent transversal fluctuations of wavelengths larger than ℓ and Eq. 9 is still valid, but with $\xi_\parallel = \ell$. If we suppose that each inclusion resides in the center of a square of length ℓ, then a simple geometrical consideration allows us to link ℓ to the surface concentration of snaps, C.

$$\ell = \sqrt{\frac{S}{N}} = \frac{1}{\sqrt{C}}, \quad (10)$$

where N is the number of snaps.

The concentration C is linked to the molar ratio R of snap-to-surfactant by the relation $C = R/a^2$ where a^2 represents the molecular area occupied by a surfactant molecule. For $C_{12}E_4$, the value of $a^2 = 42$ Å^2 (Klose et al., 1995).

Taking into account Eqs. 9 and 10 for membranes of thickness δ, the Bragg distance can be written as (G. Gompper, personal communication)

$$d_\mathrm{B} = \delta + A(\kappa, \mathrm{T})C^{-0.5}\sqrt{\arctan\left(\frac{1}{a^2 C}\right) - \arctan\left(\frac{1}{SC}\right)}, \quad (11)$$

with

$$A(\kappa, \mathrm{T}) = \sqrt{\frac{3k_{\mathrm{B}}T}{2\pi^3\kappa}}.$$

Equation 11 shows that d_{B} is a decreasing function of C and tends to δ, the thickness of the bilayer, when the concentration of inclusions increases. For high concentrations, d_{B} varies as $C^{-0.5}$ and is equivalent to the model proposed by Nicot et al. (1996). When C tends to zero, the corrective term under the root becomes preponderant, rounds up the function, and leads to a plateau for very low C values. Its origin can be easily understood because $\xi_{\|}$ should be taken as the characteristic length, as far as ℓ is lower than $\xi_{\|}$. In principle, the fitting of Eq. 11 can yield the values of δ, of the membrane rigidity κ, that of the membrane surface S, and that of the surfactant molecular area a^2. In fact, we have fixed the values of δ, determined experimentally by SAXS, and the molecular average area a^2. The fitting of experimental points by Eq. 11 allows us to calculate κ.

The Caillé exponent $\eta(d_{\mathrm{B}}, \delta)$

We have modified the classical Helfrich theory of fluctuating membranes, only by stating that a cut-off to the longest wavelength of membrane fluctuations depends on snap concentration (Eq. 11). We remain, therefore, in the Helfrich regime; indeed Helfrich (1978) has shown that, for purely steric interactions,

$$\bar{B} = \frac{9\pi^2(k_{\mathrm{B}}T)^2}{64\kappa}\frac{d_{\mathrm{B}}}{(d_{\mathrm{B}} - \delta)^4}. \tag{12}$$

Replacing $\bar{B}$ in Eq. 1 by the above expression and K by κ/d_{B}, we obtain (Roux and Safinya, 1988)

$$\eta = \frac{4}{3}\left(1 - \frac{\delta}{d_{\mathrm{B}}}\right)^2. \tag{13}$$

The fit of the SAXS spectra yields the values of η and d_{B}, while the linear fit of Eq. 13 leads to δ. It could then be expected that Eq. 13 remains valid in the presence of inclusions-snaps, as well as for bare membranes.

RESULTS AND DISCUSSION

Unbound state

In the L_α phase of the ternary system $C_{12}E_4$–dodecane–water, the membrane of thickness δ is composed of a water layer interposed between two surfactant monolayers, as depicted in Fig. 1. A characteristic SAXS spectrum of such a system is represented in Fig. 2, in both the unbound and the bound state. The broadness of the spectra originates from nonionic surfactant membranes, stabilized by the sole steric interactions. The small angle excess scattering can also be attributed to the characteristics of the system (Oda and Litster, 1997). We have calculated from these spectra the values of η, d_{B}, and δ, according to Nallet et al. (1993).

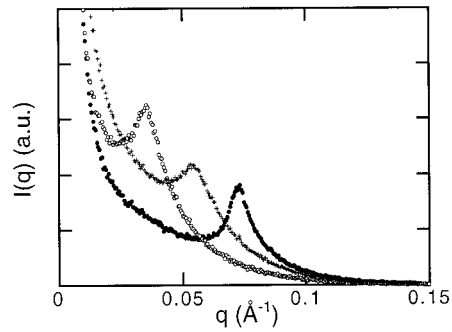

FIGURE 2 Typical SAXS spectra of lamellar phases at membrane volume fraction $\Phi = 0.28$. Bare membrane (○) and membranes decorated with snaps at increasing concentrations of peptide Leu_{12}: +, $C = 1.10^{-5}$; ●, $C = 2.5\ 10^{-5}$.

In Fig. 3, we have represented the dilution law in the unbound state, where $\Phi \cdot d_{\mathrm{B}}$ has been plotted as a function of $\ln(\Phi)$ at two water-to-surfactant volume ratios w, for surfactants $C_{12}E_4$ and $C_{10}E_4$. The fit of Eq. 2 to experimental points, for $C_{12}E_4$, leads to $\kappa = 1.5 \pm 0.2\ k_{\mathrm{B}}T$ ($1.6 \pm 0.2\ k_{\mathrm{B}}T$), and $\delta = 46$ Å (61 Å), respectively, for $w = 0.58$ ($w = 0.98$) whereas $\kappa = 0.7 \pm 0.2\ k_{\mathrm{B}}T$, and $\delta = 40$ Å for $C_{10}E_4$. The values of the bending constant of a single membrane κ, are in good agreement with those given by Sicoli et al., 1993. The membrane rigidity does not seem to vary with its thickness, although this is not always the case, as shown by Freyssingeas et al. (1996). Note that δ values using Eq. 2 are slightly lower that those deduced from SAXS experiments (Table 1). We have checked that this small discrepancy does not significantly affect the fitted κ values.

In Fig. 4, we have plotted η, the Caillé exponent, versus d_{B}^{-1}. The continuous lines are fits to Eq. 13 for the two values of membrane thickness δ. In Table 1, we compare the values of δ returned from the fit of SAXS spectra from dilution experiments and from Eq. 13. It appears, therefore,

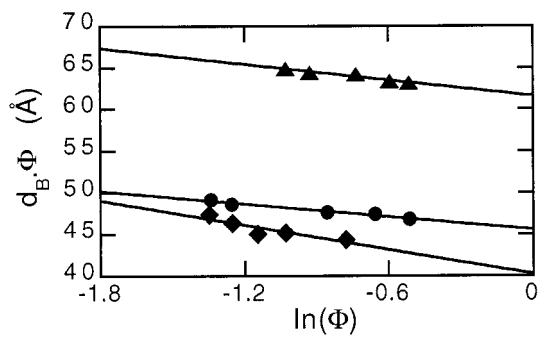

FIGURE 3 Deviation from the ideal dilution law in $C_{12}E_4$ L_α phase, for two different water-to-surfactant volume ratios: ●, $w = 0.58$, and ▲, $w = 0.98$, and in $C_{10}E_4$ L_α phase ◆, $w = 0.45$. From the linear fit to Eq. 2, one gets the membrane thickness δ (Table 1) and rigidity κ.

TABLE 1 Unbound state: membrane thickness determined from SAXS (δ_{RX}), from a fit to Eq. 2 (δ_{dil}) and from a fit to Eq. 13 (δ_η) for different water-to-surfactant ratios, *w*, and surfactants

Surfactant	*w*	δ_{RX} (Å)	δ_{dil} (Å)	δ_η (Å)
$C_{12}E_4$	0.58	53 ± 2	46 ± 1	51 ± 2
$C_{12}E_4$	0.98	64 ± 4	61 ± 1	61 ± 4
$C_{10}E_4$	0.45	49 ± 2	40 ± 1	46 ± 4

that all the results obtained in the unbound state are in very good agreement with the Helfrich theory.

Bound state

In contrast to the unbound state, where we find a relation between d_B and Φ, in the bound state, d_B does not depend anymore on Φ, but on C, the surface concentration of myelin protein, as represented in Fig. 5. The continuous line represents the fit to Eq. 11, and the experimental points carried out at several values of Φ, gather, as expected, on the same universal curve. From the fit, we obtain $\kappa = 2.8 \pm 0.4\ k_BT$ for both values of membrane thickness δ, instead of $\approx 1.5\ k_BT \pm 0.2$ for bare membranes. The values of κ have been obtained by two complementary approaches. For the unbound state, it was determined by a classical method, i.e., the correction of the dilution law (see Eq. 2), whereas, for the bound state, the value of κ was deduced from Eq. 11. Because the relation between $\xi_\perp$ and d (Eq. 8) remains still a matter of discussion, the difference between the two values of κ may not be too significant.

It should be noted that Eq. 11 describes the variation of d_B with concentration of inclusion-snaps, but not with their geometry. Indeed, when the length of the hydrophobic part of the inclusion d_π (Table 2) exceeds the length of the aliphatic part of the bilayer, it is expected according to Fig. 1 that, with the increase of C, d_B will tend to $\delta + \delta_\pi$, where δ_π represents the length of the inclusion remaining in contact with oil. This is indeed observed in Fig. 5, where $\delta_\pi = d_\pi - 16 = 26$ Å. For a membrane thickness of 51 Å, the asymptote of the curve d_B versus C, reaches a value of $\delta + \delta_\pi = 77$ Å, in good agreement with the value of δ_π. As a consequence, Eq. 11, which extrapolates to δ for high values of C, does not apply anymore for very high values of inclusion concentration. In brief, Eq. 11 is valid for $C \leq 5.10^{-5}$, this value being close to the solubility limit of the myelin proteolipid in the system.

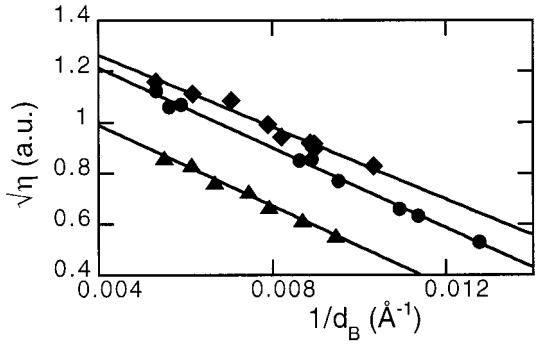

FIGURE 4 Variation of $\sqrt{\eta}$ vs. $1/d_B$. From the linear fit to Eq. 13, the membrane thickness is obtained (Table 1). Symbols are the same as in Fig. 3.

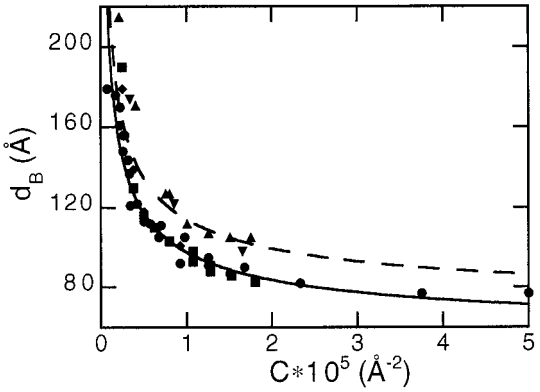

FIGURE 5 Variation of d_B vs. the myelin proteolipid concentration, C, the surface concentration of snaps, at two different values of membrane thickness and at different Φ values: ▼, $\delta = 64$ Å and $\Phi = 0.20$; ▲, $\Phi = 0.26$; ●, $\delta = 51$ Å and for $\Phi = 0.27$; ■, 0.12, ◆, and 0.19, respectively. The curves are fits to Eq. 11.

To obtain further information about the inclusion-snap mechanism, we have explored the behavior of a series of synthetic peptides, designed to form spontaneously stable α-helices in the hydrophobic domain of bilayers, with a perpendicular orientation to the plane of the membrane (Huschilt et al., 1989; Zhang et al., 1995; Deber and Li, 1995). In Fig. 6, we observe that, for peptides $(Leu)_{16}$ and $(Leu)_{12}$, the Bragg distance d_B, decreases as a function of C, the snap concentration, in a manner identical to that obtained in Fig. 5 for the four-α-helix bundle of the myelin proteolipid. In contrast, for the analog but shorter peptide $(Leu)_8$, d_B remains unchanged whatever the peptide concentration. The less hydrophobic peptides: (Ala-Leu 18) and $(Ile\text{-}Ala)_4$, do not affect the Bragg distance, although the

TABLE 2 Characteristics of hydrophobic peptide models

Snap	Length of Hydrophobic α-Helices: d_π (Å)	Hydrophobicity Scale*	Snapping Effect
Myelin proteolipid	42	N.D.	Yes
(Ala-Leu 18)	27	0.703	No
$(Leu)_{16}$	24	0.779	Yes
$(Leu)_{12}$	18	0.763	Yes
$(Leu)_8$	12	0.738	No
$(Ile\text{-}Ala)_4$	12	0.728	No

*Calculated from the mean fractional area loss according to Lesser et al. (1987)

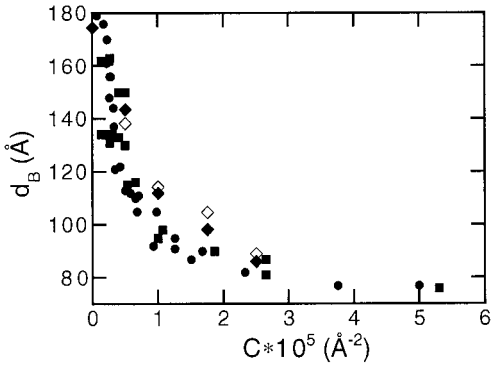

FIGURE 6 Universal behavior of d_B vs. C. All the points gather on the same curve. $C_{12}E_4$ L_α phase: ●, myelin proteolipid; ■, Leu_{16}; and ◆, Leu_{12}. $C_{10}E_4$ L_α phase: ◇, Leu_{12}.

length of (Ala-Leu 18) seems sufficient to span the bilayer. These results are summarized in Table 2: it appears that the complete crossing of the bilayer requires not only a sufficient peptide length, but also includes a hydrophobicity threshold (Liu and Deber, 1997), as illustrated by peptide (Ala-Leu 18). In contrast to zwitterionic lipidic membranes, where Liu and Deber, (1997) have observed a transmembrane insertion of (Ala-Leu 18), the latter peptide does not seem to span a nonionic bilayer by a spontaneous hydrophobic mechanism. This is confirmed by the use of a hydrophobicity scale based on the mean fractional area loss by residue (Lesser et al., 1987). From Table 2, it is obvious that, for any value under about 0.750, a peptide cannot function as an active snap.

As for the unbound L_α phase, we have plotted the Caillé exponent $\sqrt{\eta}$ versus d_B^{-1}, after incorporation of molecular snaps. Remember that, in contrast to the unbound lamellar phase, the variation of d_B does not originate anymore from Φ, but from C, the concentration of the snaps. As illustrated in Fig. 7, the relation is linear, indicating that Eq. 13 is still

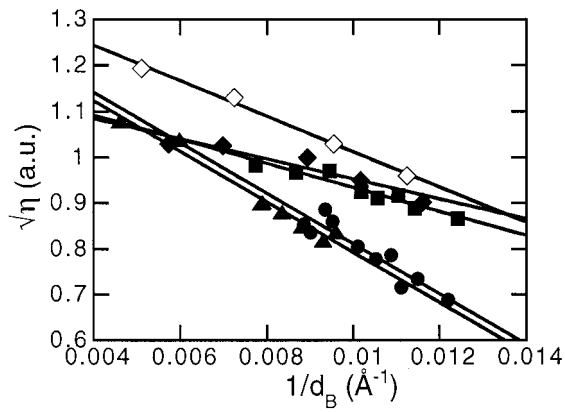

FIGURE 7 Variation of $\sqrt{\eta}$ vs. $1/d_B$. $C_{12}E_4$ L_α phase: δ = 64 Å: ▲, myelin proteolipid. δ = 51 Å: ●, myelin proteolipid; ■, Leu_{16}; and ◆, Leu_{12}. $C_{10}E_4$ L_α phase: ◇, Leu_{12} and δ = 46 Å. The lines are fits to Eq. 13 (Table 3).

valid under these conditions. However, in presence of molecular snaps, the picture is completely different: the results, summarized in Table 3, reveal that δ does not correspond anymore to the thickness of the membrane. For example, if we consider the two membranes of thickness 51 Å and 64 Å, after insertion of the myelin proteolipid, the value of δ_η obtained from the fit of Eq. 13, is 41 Å. If, now, we consider the behavior of peptide snaps of various lengths, the values of δ_η are close to d_π. They correspond to the length of their hydrophobic sequences, and remain independent of the membrane thickness δ. It appears, therefore, that, under such conditions, interlamellar interactions cannot be described anymore in terms of sole steric interactions: we have to take into consideration the effect of macromolecular inclusions.

On the phenomenological level of description, the expression of $\bar{B}$ in Eq. 12, remains valid for results involving molecular snaps. It is worthwhile to note that, whereas, for an unbound lamellar phase stabilized by Helfrich interactions, δ represents the membrane thickness, for the bound lamellar phase we observe that $\delta \approx d_\pi$, i.e., the length of the α-helical hydrophobic part of the protein or peptide snap. Therefore, it is, not surprizing that its contribution appears in the expression of $\bar{B}$, describing the interactions between membranes. In Fig. 8, we represent experimental $\bar{B}$ values deduced from Eq. 1 for three types of snaps, using the value of κ obtained by fitting Eq. 11 and the value η obtained by fitting the x-ray spectra. The solid line in Fig. 8 represents the variation of $\bar{B}$ with d_B given by Eq. 12, where δ is the membrane thickness and $\kappa \approx 2\ k_BT$. The dashed curves have been obtained using Eq. 12, but replacing δ by δ_π, the length of the hydrophobic snaps.

For a given value of d_B, we observe that the presence of snaps decreases the values of $\bar{B}$ and that the variation is more important for shorter snaps. This result can be understood by reference to Fig. 9, where three different situations are represented for the same average distance between the membranes. $\bar{B}$ is related through Eq. 12 to d_B for the bare membrane (Fig. 9 *A*). In the presence of longer snaps (Fig. 9*B*), the space available for membrane fluctuation is locally increased, leading to the local decrease of interactions between the membranes, and, at the same time, of $\bar{B}$. This

TABLE 3 Bound state: membrane thickness as determined from SAXS (δ_{RX}) and from a fit to Eq. 13 (δ_η). Comparison with the calculated hydrophobic length of different snaps (d_π). Obviously $\delta_\eta \approx d_\pi$

Surfactant	Molecular Snap	δ_{RX} (Å)	δ_η (Å)	d_π (Å)
$C_{12}E_4$				
	Myelin proteolipid	64 ± 4	41 ± 3	42
		51 ± 2	41 ± 4	42
	$(Leu)_{16}$	52 ± 1	22 ± 3	24
	$(Leu)_{12}$	51 ± 3	19 ± 4	18
$C_{10}E_4$	$(Leu)_{12}$	46 ± 1	27 ± 3	18

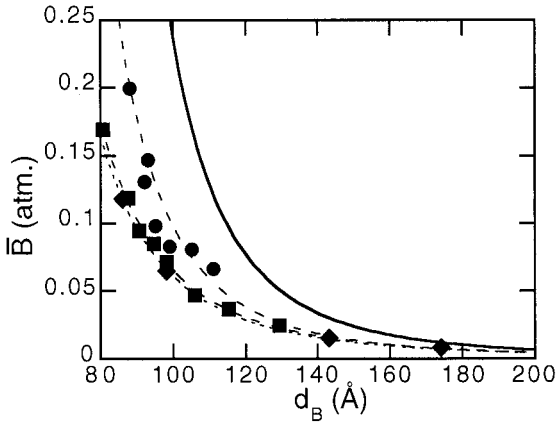

FIGURE 8 Variation of $\bar{B}$ vs. the lamellar period in $C_{12}E_4$ lamellar phase decorated with ●, myelin proteolipid, ■, Leu_{16}, and ◆, Leu_{12}. Dashed curves are obtained using Eq. 12 with $\delta = d_\pi$, whereas the solid curve corresponds to bare L_α where δ is the membrane thickness. Note that, for a fixed d_B value, $\bar{B}$ decreases when the hydrophobic length of the snap decreases.

situation is enhanced in Fig. 9 *C* because the local distance between the membranes is further increased when the length of the snap is decreased.

Determination *ab initio* of the snap contribution in the interaction term would be, in fact, the next logical step, but its solution remains, up to now, very arduous in our hands. Recently, several investigators have suggested models for membrane inclusions, starting with an expression of the Hamiltonian of the lamellar phase decorated with snaps (Sens and Turner, 1997; Sens et al., 1997; Turner and Sens, 1999). However, they use the expression of $\bar{B}$ given by Eq. 12, and they are unable to fit correctly our experimental data.

CONCLUSION

In summary, our experimental data are in excellent agreement with a Helfrich-like theory of stacked membranes, stabilized by thermal fluctuations. In Helfrich's model of sterical interactions, the interlamellar distance d_B is a function of several parameters: the temperature T, the rigidity constant of a single membrane κ, the constant that describes the interaction between membranes $\bar{B}$, and $\xi_{\|}$, which is related to the largest fluctuation wavelength of the membrane.

Molecular snaps induce a binding transition by bridging adjacent membranes. We have postulated that the largest fluctuation wavelength of the membrane is equal to the lateral distance ℓ between snaps. Since ℓ is related to the concentration of snaps in an L_α phase, our model allows us to relate the interlamellar distance d_B to the snap concentration C. Taking this result into account, the fit to Eq. 11 is excellent and all experimental points gather on a single universal curve $d(C)$, as expected from the model.

SAXS experiments allow the determination of Caillé parameter η. In L_α phases stabilized by thermal fluctuations, $\eta^{0.5}$ decreases linearly with a slope proportional to the membrane thickness, whereas d_B increases. When snaps are present, we have verified that the linear relation is indeed still valid. However, the slope then seems independent of membrane thickness, but is instead proportional to the length of the hydrophobic part of the snap. It seems reasonable to state that when snaps are active, the interactions between membranes, and therefore $\bar{B}$, are modified. Because the slope of $\eta^{0.5}$ is due to the explicit expression of $\bar{B}$, we have modified it in a heuristic manner to fit our experimental data.

The interplay between the hydrophobic properties and the length of the peptide sequence has allowed us to identify and to optimize the size of α-helices and their hydrophobicity scale, prerequisite for bilayer penetration and snap-like effect (Table 2). In the absence of surfactant charges, the studied phenomenon indicates the importance of hydrophobic driving forces in bilayer insertion of peptides and in the conformational stability of transmembrane proteins (Merdas et al., 1998). Such effects may be operative in the protein scaffolding mechanism suggested for the proteolipid function in native myelin (Edwards et al. 1989).

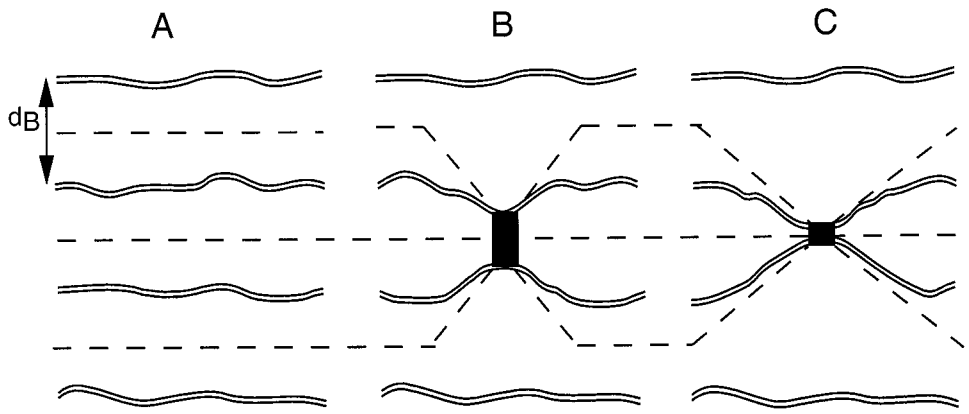

FIGURE 9 Diagram of the space available for membrane fluctuation in the vicinity of a snap bridging two membranes, at an identical d_B value. (*A*) Fluctuating bare membrane; dotted lines represents roughly the amplitude of the membrane fluctuation. When the length of the snap decreases (*B* and *C*), the space available for the upper and lower membranes increases locally; this leads to the decrease of interactions between membranes.

We are aware that many questions remain to be addressed concerning biopolymers inserted in lamellar phases. For example, what is the effect of physicochemical properties of the inclusion, such as charge, volume, and hydrophobicity on membrane flexibility? We expect that our results will contribute to the elucidation of these questions and ultimately provide a clearer understanding of a number of membrane-vital mechanisms (rigidity, fusion, pore creation, etc.). In addition, practical results may ensue from such studies: for example, more efficient drug delivery systems and/or new materials of therapeutic importance.

This work has been supported in part by Centre National de la Recherche Scientifique (Physique et Chimie du vivant) and a grant from the Simone et Gino Del Duca Fundation.

The authors acknowledge the work of P. D. Semchuk for obtaining (Ile-Ala)$_4$, (Leu)$_{12}$, and (Leu)$_{16}$ peptides and P. Sens, G. Gompper, and J. Meunier for stimulating discussions.

REFERENCES

Abney, J. R., and J. C. Owicki. 1985. Theories of protein–lipid and protein–protein interactions in membranes. *In* Progress in Protein–Lipid Interactions. A. Watts and J. J. H. H. M. de Pont, editors. Elsevier Science Publishers, Amsterdam, The Netherlands. 1–59.

Bouglet, G., and C. Ligoure. 1999. Polymer-mediated interactions of fluid membranes in a lyotropic lamellar phase: a small angle x-ray and neutron scattering study. *Eur. Phys. J. B.* 9:137–147.

Brooks, J. T., and M. E. Cates. 1993. The role of added polymer in dilute lamellar surfactant phases. *J. Chem. Phys.* 99:5467–5480.

Caillé, A. 1972. Physique Cristalline. *C. R. Acad. Sci. Paris.* 274:891–893.

Cantor, C., and P. Schimmel, 1980. Biophysical Chemistry. Part 1: The Conformation of Biological Macromolecules. W. H. Freeman and Co., New York.

Daoud, M., and P. G. de Gennes. 1977. Statistic of macromolecular solutions trapped in small pores. *J. Phys. France.* 38:85–93.

Davis, H., D. M. Clare, R. S. Hodges, and M. Bloom. 1983. Interaction of a synthetic amphiphilic polypeptide and lipids in a bilayer structure. *Biochemistry.* 22:5298–5305.

Deber, C. M., and S. C. Li. 1995. Peptides in membranes: helicity and hydrophobicity. *Biopolymers (Peptide Sci.).* 37:295–318.

Edwards, A. M., N. W. Ross, J. B. Ulmer, and P. E. Braun; 1989. Interaction of myelin basic protein and proteolipid protein. *J. Neurosci. Res.* 22:97–102.

Freyssingeas, E., D. Roux, and F. Nallet. 1996. The effect of water thickness on the bending rigidity of inverted bilayers. *J. Phys. Condens. Matter.* 8:2801–2806.

De Gennes, P. G. 1974. The Physics of Liquid Crystals. Oxford University Press, Oxford, U.K. 273–325.

Golubovic, L., and T. Lubensky. 1989. Smectic elastic constants of lamellar fluid membrane phases: crumpling effects. *PRB.* 39:12110–12133.

Gompper, G., and M. Schick. 1994. Self-Assembling Amphiphilic Systems. Phase Transitions and Critical Phenomena. vol 16. Academic Press, New York. 139–141.

Greer, J. M., R. A. Sobel, A. Sette, S. Southwood, M. B. Lees, and V. K. Kuchroo. 1996. Immunogenic and encephalitogenic epitope clusters of myelin proteolipid protein. *J. Immunol.* 156:371–379.

Helfrich, W. 1978. Steric interaction of fluid membranes in multilayer systems. *Z. Naturforsch.* 33a:305–315.

Helfrich, W., and R. M. Servuss. 1984. Undulations, steric interaction and cohesion of fluid membranes. *Il nuovo cimento.* 3D:137–151.

Helfrich, W. 1985. Effect of thermal undulations on the rigidity of fluid membranes and interfaces. *J. Phys.* 46:1263–1268.

Honig, B., and A. Nicholls. 1995. Classical electrostatics in biology and chemistry. *Science.* 268:1144–1149.

Huschilt, J. C., B. M. Millman, and J. H. Davis. 1989. Orientation of α-helical peptides in lipid bilayers. *Biochim. Biophys. Acta.* 979:139–141.

Klose, G., S. Eisenblätter, J. Galle, A. Islamov, and U. Dietrich. 1995. Hydration and structural properties of a homologous series of nonionic alkyl oligo (ethylene oxide) surfactants. *Langmuir.* 11:2889–2892.

Kunieda, H., K. Nakamura, H. T. Davis, and D. F. Evans. 1991. Formation of vesicles and microemulsions in a water, tetraethylene glycol dodecyl ether/dodecane. *Langmuir.* 7:1915–1919.

Leibler, S., and R. Lipowsky. 1987. Complete unbinding and quasi-long-range order in lamellar phases. *PRB.* 35:7004–7009.

Lei, L., C. R. Safinya, and R. F. Bruisma. 1995. Discrete harmonic model for stacked membranes: theory and experiment. *J. Phys. II France.* 5:1155–1163.

Lesser, G. J., R. H. Lee, M. H. Zehfus, and G. D. Rose. 1987. Hydrophobic interactions in proteins. *In* Protein Engineering. Alan R. Liss Inc. New York. 175–179.

Liu, L. P., and C. M. Deber. 1997. Anionic phospholipids modulate peptide insertion into membranes. *Biochemistry.* 36:5476–5482.

Marcelja, C. 1999. Toward a realistic theory of the interaction of membrane inclusions. *Biophys. J.* 76:593–594.

Merdas, A., M. Gindre, R. Ober, C. Nicot, W. Urbach, and M. Waks. 1996. Nonionic surfactant reverse micelles of $C_{12}E_4$ in dodecane: temperature dependence of size and shape. *J. Phys. Chem.* 100:15180–15186.

Merdas, A., M. Gindre, J.-Y. Le Huérou, R. Ober, C. Nicot, W. Urbach, and M. Waks. 1998. Bridging of nonionic reverse micelles by a myelin transmembrane protein. *J. Phys. Chem. B.* 102:528–533.

Nallet, F., R. Laversanne, and D. Roux. 1993. Modelling x-ray or neutron scattering spectra of lyotropic lamellar phases: interplay between form and structure factors. *J. Phys. II France.* 3:487–502.

Nicot, C., M. Waks, R. Ober, T. Gulik-Krzywicki, and W. Urbach. 1996. Squeezing of oil-swollen surfactant bilayers by a membrane protein. *PRL.* 77:3485–3488.

Oda, R., and J. D. Litster. 1997. Effect of symmetry on a three-component lamellar phase: x-ray scattering study. *J. Phys. II France.* 7:815–824.

Roux, D., and C. R. Safinya. 1988. A synchrotron x-ray study of competing undulation and electrostatic interlayer interactions in fluid multimembrane lyotropic phases. *J. Phys. France.* 49:307–318.

Roux, D., F. Nallet, E. Freyssingeas, G. Porte, P. Bassereau, M. Skouri, and J. Marignon. 1992. Excess area in fluctuating-membrane systems. *Eur. Phys. Lett.* 17:575–581.

Sens, P., and M. S. Turner. 1997. Inclusions in thin smectic films. *J. Phys. France II.* 7:1855–1870.

Sens, P., M. S. Turner, and P. Pincus. 1997. Particulate inclusion in a lamellar phase. *PRE.* 55:4394–4408.

Sereda, T., C. Mant, A. Quinn, and R. S. Hodges. 1993. Effect of the α-amino group on peptide retention behaviour in reversed-phase chromatography. *J. Chromatogr.* 646:17–30.

Sicoli, F., D. Langevin, and L. T. Lee. 1993. Surfactant film bending elasticity in microemulsions: structure and droplet polydispercity. *J. Chem. Phys.* 99:4759–4765.

Turner, M. S., and P. Sens. 1999. Inclusions on fluid membranes anchored to elastic media. *Biophys. J.* 76:564–572.

Vacher, M., M. Waks, and C. Nicot. 1989. Myelin proteins in reverse micelles: tight lipid association required for insertion of the Folch-Pi proteolipid into a membrane-mimetic system. *J. Neurochem.* 52: 117–123.

Weimbs, T., and W. Stoffel. 1992. Proteolipid protein (PLP) of CNS myelin: positions of free, disulfide-bonded and fatty acid thioester-linked cystein residues and implications for the membrane topology of PLP. *Biochemistry.* 31:12289–12296.

Zhang, Y. P., R. N. A. H. Lewis, G. D. Henry, B. D. Sykes, R. S. Hodges, and R. N. McElhaney. 1995. Peptide model of helical hydrophobic transmembrane segments of membrane proteins. *Biochemistry.* 34: 2348–2361.